Int. J. Heat Mass Transfer. Vol. 12, pp. 333–347. Pergamon Press 1969. Printed in Great Britain

HEAT TRANSFER BY SIMULTANEOUS CONDUCTION AND RADIATION FOR TWO ABSORBING MEDIA IN INTIMATE CONTACT†

L. A. TARSHIS‡, S. O'HARA§ and R. VISKANTA‖
General Electric Research and Development Center, Schenectady, New York

(*Received* 7 *May* 1968 *and in revised form* 19 *September* 1968)

Abstract—Energy transfer by simultaneous conduction and radiation between two media in an intimate contact is considered with principle emphasis on the mathematical formulation of the radiative flux. To gain some insight into the effects introduced by radiative transfer, the formidable general problem is simplified to one-dimensional, steady-state, diffusion between two partially transparent media in intimate thermal contact. The numerical method of solution for the resulting coupled, non-linear, integro-differential equations is described in detail. The results are presented as a series of dimensionless temperature and corresponding flux distributions for a variety of optical and physical properties. Interpretation of these results is given both on the basis of physical reasoning and relative to the mathematical formulation.

NOMENCLATURE

Note that a subscript j, in all cases, indicates the particular quantity in either media.

c_j, specific heat (per unit weight);
E_{bj}, $= \sigma T_j^4$;
$E_n(s)$, exponential integral function of order n of argument s;
F_j, net radiative flux;
G_c, irradiation on the solid/gas interface coming from chamber;
J_j, radiant energy flux leaving the interface;
k_j, thermal conductivity;
L_S, crystal length;
L_L, thermal layer thickness;
L_∞, length of bulk fluid bath;
N, $= n_\infty^2 \sigma T_\infty^3/(k_\infty/L_S)$;
n_j index of refraction;
q_j net flux;
r_{ij}, reflectance of interface between media i and j;
t_{ij}, transmittance of interface between media i and j $(t_{ij} + r_{ij} = 1)$;
T_c, steady chamber temperature;
T_j, temperature;
T_M, equilibrium melting temperature;
T_∞, far field bath temperature;
u_j, fluid velocity;
x, y, z, Cartesian coordinates.

Greek symbols

α, absorptance;
β, η, ζ, ψ, dummy variables of integration;
ϵ, emittance;
θ_j, T_j/T_∞;
θ_M, T_M/T_∞;
$\varkappa_j$, spectral absorption coefficient;
ρ_j, density;
σ, Stefan–Boltzmann constant;

† This paper is based on part of the dissertation submitted by L. A. Tarshis in partial fulfillment of the Ph.D. requirements of the Materials Science Department, Stanford University.

‡ Formerly with the Dept. of Materials Science, Stanford University, Stanford, California.

§ Research Associate, Dept. of Materials Science, Stanford University, Stanford, California.

‖ Professor of Mechanical Engineering, Purdue University, Lafayette, Indiana.

τ, ξ, optical distances in solid and liquid respectively;
τ_j, $\varkappa_j L_j$;
τ_∞ $= \varkappa_\infty L_\infty$.

For definition of starred quantities see Table 2.

1. INTRODUCTION

PRIMARILY due to mathematical complexities, it has been common practice in engineering to neglect transfer by radiation, especially in condensed phases (solid and liquid), and to determine the temperature distribution and heat fluxes on the basis of conduction and/or convection alone. This assumption has usually been quite valid based on the fact that most materials of engineering application are either

(i) used at relatively low temperatures where the radiant emission is small or
(ii) absorb most radiant energy within a few atomic layers of the surface.

The latter is especially true for metals whose optical absorption frequencies generally correspond to the frequencies of the emitted thermal radiation. However, in the more general realm of materials science, there are numerous materials which are, to various degrees, transparent to thermal radiation. In this category of materials are those substances used in optical lasers, e.g. ruby, sapphire, etc. When these materials are used at or near their relatively high melting temperatures, the radiant flux is not at all negligible compared to conductive or convective fluxes since very little thermal energy is actually absorbed by these molecules.

It has only been within recent years that these problems of simultaneous heat transfer by different modes have been considered quantitatively with the principle application being to the radiation emitting, absorbing, and scattering nature of the gas phase. Numerical solutions to the general conservation equation have been obtained, for certain simplified cases, in homogeneous matter and have provided much insight into the general problem of energy transport. No solutions have been reported for simultaneous transfer for more than one absorbing and emitting medium in intimate thermal contact.

The initial motivation for this study was to predict the temperature distributions and corresponding thermal fluxes during the crystal growth of semi-transparent materials. Such information is essential in understanding the nature of solidification as well as in the actual control of the growth process. Therefore, such a situation has been modeled, mathematically, and the more general results for any two contacting absorbing media experiencing coupled radiative and conductive heat transport are presented.

2. MATHEMATICAL FORMULATION

This section is divided into three parts. In the first part, the generalized energy equations for the two media are derived, relative to a physical model, including some possible boundary conditions for two partially transparent, adjoining, media. In the second portion, the details for the particular example which we will solve are described. Lastly, the numerical procedure successfully used for solution are outlined.

(a) *Energy equations*

The physical model and corresponding coordinate system are shown in Fig. 1. Material I is in perfect thermal contact with material II across the stationary plane $x = z = 0$; the former extending in the positive x direction to $x = L_{\mathrm{I}}$, the latter in the positive z direction to $z = L_{\mathrm{II}}$. For the time being, the configuration is assumed to be finite in width (y direction) and the conditions on the ends are neglected. Considering the most general case of simultaneous conduction, convection, and radiation, the equation of conservation of thermal energy within either media may be written:

$$c_j \rho_j \frac{\partial T_j}{\partial t} = \nabla \cdot [k_j \nabla T_j - c_j \rho_j u_j T_j - F_j]; \quad j = \mathrm{I}, \mathrm{II} \qquad (1)$$

where the three terms in the brackets are the conductive, convective and radiative fluxes respectively in the jth phase. In these equations k_j is the appropriate thermal conductivity; ρ_j the density; c_j the specific heat; T_j the absolute temperature; u_j the fluid velocity vector, and F_j the local radiative flux. As such, the solution to equation (1) is untenable and two immediate simplifications are made. The first is to assume that the steady state has been achieved and therefore $\partial T_j/\partial t = 0$. As a result, one may obtain†

$$k_j \nabla^2 T_j - c_j \rho_j u_j \nabla T_j - \nabla . F_j = 0; \quad j = \text{I, II}. \qquad (2)$$

The second assumption, and probably the more critical, is to assume that lateral heat transport is of negligible importance. This is equivalent to assuming that the media described in Fig. 1 are infinitely wide ($-\infty < y < \infty$). These assumptions reduce the problem to a steady, one-dimensional, heat transfer analysis defined by the equation:

$$\frac{d}{dx_j}\left[k_j \frac{dT_j}{dx_j} - c_j \rho_j u_j T_j - F_j\right] = 0; \quad j = \text{I, II} \qquad (3)$$

with the particular parameters defined in the proper media. Integrating equation (3) once with respect to distance, x_j:

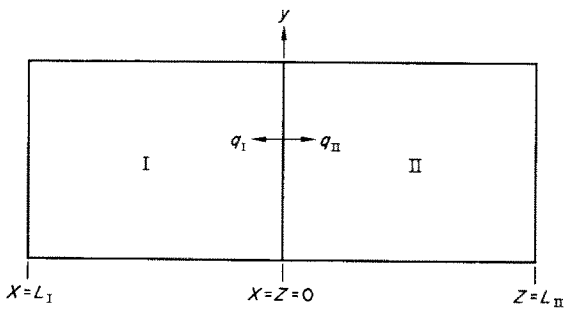

FIG. 1. Schematic of two media in intimate thermal contact.

$$k_j \frac{dT_j}{dx_j} - c_j \rho_j u_j T_j - F_j = -q_j; \quad j = \text{I, II} \qquad (4)$$

where q_j is a constant total energy flux in the media. Furthermore, it has been assumed that, in the problem to be treated, the spectral absorption coefficient is independent of the wavelength of the radiation. Such an assumption is again necessary to make the equation tractable. However, an example in which this assumption would be valid corresponds to the case of sapphire (Al_2O_3) near its melting temperature. These simplifications, although limiting, permit mathematical solution and the results should still provide adequate insight into the general problem. Independent of the conditions elsewhere in the media, two boundary conditions must always be met at the interface. These are conservation of heat and continuity of temperature resulting from the assumption of intimate contact. In terms of q_j, the net energy flux in the respective positive directions in each material, these interface conditions yield:

$$q_I = -q_{II} \qquad (5)$$

and

$$T_I = T_{II} \qquad (6)$$

both applied at $x = z = 0$. With the lengths L_{II} and L_I fixed and interface conditions, equations (5) and (6), required, it is only necessary to impose two additional boundary conditions to completely specify the solution to equation (4). There are many such possible constraints dependent on the physical system under consideration. Among these are:

(i) The interface temperature is known.
(ii) The temperature at either end is a known constant.
(iii) Flux conservation conditions at the ends.

With these conditions in mind, we now turn to the evaluation of the radiative fluxes, F_j, in either media.

Since radiative transfer methods are well known [1, 2], the lengthy mathematical details

† Implicitly assumed in writing equation (1) is that ρ_j and c_j are constant. Therefore it follows that $\nabla . u_j = 0$.

of the derivation are not repeated here. As is convenient for all radiation problems, the optical distances are defined as:

$$\tau_{\mathrm{I}} = \int_0^x \varkappa_{\mathrm{I}}\,\mathrm{d}x \quad \text{for material I } (0 < x \leqslant L_{\mathrm{I}}) \qquad (7a)$$

and

$$\tau_{\mathrm{II}} = \int_0^z \varkappa_{\mathrm{II}}\,\mathrm{d}z \quad \text{for material II } (0 < z \leqslant L_{\mathrm{II}}) \qquad (7b)$$

where $\varkappa_j$ is the absorption coefficient. It can be shown [2] that the amount of radiant flux emitted at a point η which actually reaches the plane of interest (corresponding to τ) may be generally written:

$$n_j^2\, E_{bj}(\eta)\,[2E_2(|\tau - \eta|)] \qquad (8)$$

where n is the index of refraction, $E_{bj}(\eta)$ is the black body emissive power given by Stefan–Boltzmann law ($E_{bj} = \sigma T_j^4$); and $E_n(x)$ is the tabulated exponential integral function defined as:

$$E_n(x) = \int_0^1 \psi^{n-2} \exp(-x/\psi)\,\mathrm{d}\psi = \int_1^\infty \beta^{-n} \exp(-x\beta)\,\mathrm{d}\beta. \qquad (9)$$

The appearance of the exponential integral function, which is more slowly damping than the exponential function, can be understood physically by noting that radiation from all angles to the single axis of interest contributes to radiation intensity at any point in contrast to the simpler case of uni-directional radiation.

Little additional insight into the effects of radiative heat transport can be gained at this point by continuing the general procedure. It proves much more informative to treat a specific example where the problem may be solved and the results evaluated. The mandatory assumptions which are made also serve to point out the limitations of the present analysis and, in some cases, suggest areas for further investigation.

(b) *Specific example*

For illustrative purposes and for obtaining a solution, the physical model in Fig. 1 is modified to that given in Fig. 2. This would be typical of an infinite diameter crystal in thermal equilibrium with its melt. The upper surface of the crystal exchanges radiant energy with a chamber at constant temperature T_c. The media between the upper crystal surface and the chamber can, in general, be any inert gas but for simplicity we assume it to be a vacuum. The irradiation of the solid/gas interface due to radiation leaving the chamber walls is G_c. The solid/liquid interface temperature is assumed to be the equilibrium melting temperature, T_M. Since the primary interest is in the effects caused by radiation, the complicated details introduced by convective transport are neglected. The bulk bath is assumed to be efficiently mixed so as to maintain the liquid at constant temperature (T_∞) up to a distance L_L (the thermal layer) from the solid/liquid interface. Within the thermal layer, convective transport is assumed negligible† or, equivalently,

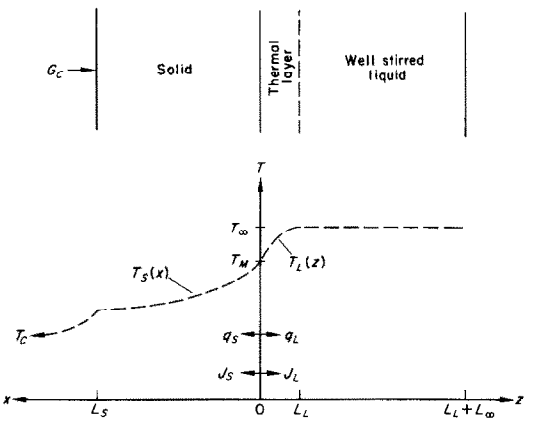

FIG. 2. Physical model and schematic of the corresponding temperature distribution for a solid phase in thermodynamic equilibrium with its melt.

† This assumption would hold for the case of a rotating crystal in which the forced convection just overcomes the natural convection flow in the opposite direction.

$u = 0$. The following assumptions have also been made in this analysis.

(1) Scattering is negligible compared to absorption.
(2) Interreflections of radiation between the liquid/solid and solid/gas interfaces are negligible.
(3) Reflection and transmission of radiation at the liquid/solid interface and transmission at the solid/gas interface are diffuse.
(4) Both media are assumed gray, i.e., the spectral absorption coefficients have been averaged over the entire wavelength spectrum and replaced by a Planck mean. As a result, the optical distances are defined as the products of the absorption coefficients and the distance of the plane of interest from the interface. Therefore $0 < \xi \leqslant \tau_L = \varkappa_L L_L$ and $0 < \tau \leqslant \tau_S = \varkappa_S L_S$. ($\xi$ is the optical distance in the liquid and corresponds to τ in the solid.).
(5) The index of refraction in each phase is assumed constant with respect to variations of temperature, wavelength, etc.
(6) The thermal conductivities are assumed independent of temperature.
(7) The radiation properties of the interfaces are independent of direction; e.g. $t_{LS} = t_{SL}$ where t_{ij} represent the transmittance going from the ith phase to the jth.

By considering all of the possible sources of radiative flux consistent with our model, the radiative flux in the solid (positive x-direction) is seen to be:

$$F_S(\tau) = 2[\int_0^{\tau} n_S^2 E_{bS}(\eta)\, E_2(\tau - \eta)\, d\eta - \int_{\tau}^{\tau_S} n_S^2 E_{bS}(\eta)\, E_2(\eta - \tau)\, d\eta + J_S E_3(\tau) - t_{GS} G_c E_3(\tau_S - \tau)] \quad (10a)$$

where the radiative flux crossing the liquid/solid interface in the positive x-direction, J_S, is defined as:

$$J_S = 2\{t_{LS}[\int_0^{\tau_L} n_L^2 E_{bL}(\zeta)\, E_2(\zeta)\, d\zeta + \int_{\tau_L}^{\tau_L+\tau_\infty} n_\infty^2 E_{b\infty}(\zeta)\, E_2(\zeta)\, d\zeta] + r_{LS}[\int_0^{\tau_S} n_S^2 E_{bs}(\eta)\, E_2(\eta)\, d\eta + t_{GS} G_c E_3(T_S)]\}. \quad (10b)$$

In these equations it is clear that $\tau_\infty = \varkappa_\infty L_\infty$; E_{bj} is the black body emissive power in the jth phase; t_{LS} represents the transmittance of the solid/liquid interface; r_{LS} the corresponding reflectance ($t_{LS} + r_{LS} = 1$); and the t_{GS} the transmittance of the gas/solid interface.

In direct analogy to the above, the radiative flux in the liquid phase (positive z-direction) is given by:

$$F_L(\xi) = 2[\int_0^{\xi} n_L^2 E_{bL}(\zeta)\, E_2(\xi - \zeta)\, d\zeta - \int_{\xi}^{\tau_L} n_L^2 E_{bL}(\zeta)\, E_2(\zeta - \xi)\, d\zeta + J_L E_3(\xi) - \int_{\tau_L}^{\tau_L+\tau_\infty} n_\infty^2 E_{b\infty}(\zeta)\, E_2(\zeta - \xi)\, d\zeta] \quad (11a)$$

where J_L, the radiative flux crossing the solid/liquid interface in the positive z-direction, is defined as:

$$J_L = 2\{t_{SL}[\int_0^{\tau_S} n_S^2 E_{bs}(\eta)\, E_2(\eta)\, d\eta + t_{GS} G_c E_3(\tau_S)] + r_{SL}[\int_0^{\tau_L} n_L^2 E_{nL}(\zeta)\, E_2(\zeta)\, d\zeta + \int_{\tau_L}^{\tau_L+\tau_\infty} n_\infty^2 E_{b\infty}(\zeta)\, E_2(\zeta)\, d\zeta]\}. \quad (11b)$$

It has been implicitly assumed in the above flux equation for the liquid that the bulk bath is optically thick so as to neglect reflections from $\xi = \tau_L + \tau_\infty$. Since the temperature in the completely mixed fluid (denoted by the subscript ∞) is constant, the integrals involving $E_{b\infty}$ can readily be evaluated yielding:

$$\int_{\tau_L}^{\tau_L+\tau_\infty} n_\infty^2 E_{b\infty}(\zeta)\, E_2(\zeta - \xi)\, d\zeta = n_\infty^2 E_{b\infty}[E_3(\tau_L - \xi) - E_3(\tau_L + \tau_\infty - \xi)] \quad (12)$$

which can be substituted in equations (10) and (11).

It proves convenient, in presenting the results, to introduce dimensionless variables. These are presented in Table 1. Note, that the conditions in the well-mixed liquid (denoted by subscript ∞) were arbitrarily selected as reference. The conservation of energy in the bulk media are thereby expressed, from equation (4):

$$\tau_S k_S^* \frac{\mathrm{d}\theta_S}{\mathrm{d}\tau} = -q_S^* + NF_S^*(\tau) \tag{13}$$

and

$$\tau_L \frac{\mathrm{d}\theta_L}{\mathrm{d}\xi} = -q_L^*\left(\frac{L_L}{L_S}\right) + N\left(\frac{L_L}{L_S}\right) F_L^*(\xi). \tag{14}$$

The required boundary conditions for this specific example become:

$$q_S^* = -q_L^* \tag{15a}$$

$$\theta_S = \theta_L = \theta_M \quad \text{at} \quad x^* = z^* = 0 \tag{15b}$$

$$\theta_L = 1 \quad \text{at} \quad z^* = 1. \tag{15c}$$

In dimensionless notation the radiation fluxes are expressed by:

$$F_S^*(\tau) = 2[n_S^{*2} \int_0^{\tau} \theta_S^4(\eta)\, E_2(\tau - \eta)\, \mathrm{d}\eta - n_S^{*2} \int_{\tau}^{\tau_S} \theta_S^4(\eta)\, E_2(\eta - \tau)\, \mathrm{d}\eta + J_S^* E_3(\tau) - t_{GS} G_c^* E_3(\tau_S - \tau)] \tag{16a}$$

where

$$J_S^* = 2\{t_{LS}[\int_0^{\tau_L} \theta_L^4(\zeta)\, E_2(\zeta)\, \mathrm{d}\zeta + E_3(\tau_L) - E_3(\tau_L + \tau_\infty)] + r_{LS}[n_S^{*2} \int_0^{\tau_S} \theta_S^4(\eta)\, E_2(\eta)\, \mathrm{d}\eta + t_{GS} G_c^* E_3(\tau_S)]\} \tag{16b}$$

and for the liquid

$$F_L^*(\xi) = 2[\int_0^{\xi} \theta_L^4(\zeta)\, E_2(\xi - \zeta)\, \mathrm{d}\zeta - \int_{\xi}^{\tau_L} \theta_L^4(\zeta)\, E_2(\zeta - \xi)\, \mathrm{d}\zeta + J_L^* E_3(\xi) - E_3(\tau_L - \xi) + E_3(\tau_L + \tau_\infty - \xi)] \tag{17a}$$

Table 1, Dimensionless parameters for radiation heat transfer

$x^* = \dfrac{x}{L_S}$	$k^* = \dfrac{k}{k_\infty}$	$q^* = \dfrac{q}{k_\infty T_\infty / L_S}$
$z^* = \dfrac{z}{L_L}$	$n^* = \dfrac{n}{n_\infty}$	$F^* = \dfrac{F}{n_\infty^2 \sigma T_\infty^4}$
$\theta = \dfrac{T}{T_\infty}$	$N = \dfrac{n_\infty^2 \sigma T_\infty^3}{k_\infty / L_S}$	$J^* = \dfrac{J}{n_\infty^2 \sigma T_\infty^4}$
		$G_c^* = \dfrac{G_c}{n_\infty^2 \sigma T_\infty^4}$

where

$$J_L^* = 2[t_{SL}[n_S^{*2} \int_0^{\tau_S} \theta_S^4(\eta)\, E_2(\eta)\, \mathrm{d}\eta + t_{GS} G_c^* E_3(\tau_S) + r_{SL}[\int_0^{\tau_L} \theta_L^4(\zeta)\, E_2(\zeta)\, \mathrm{d}\zeta + E_3(\tau_L) - E_3(\tau_L + \tau_\infty)]\}. \tag{17b}$$

(c) *Method of solution of energy equations*

Each of the conservation of energy equations (equations (13) and (14)) is of the non-linear, integro-differential type; the solution of which was discussed in detail by Viskanta and Grosh [2]. Their conclusion was that the best that could be hoped for in the way of a solution was via numerical or approximate techniques. In the present problem, the solution is further complicated by the fact that the two conservation equations are coupled via the interface boundary conditions. Due to the radiative heat transfer, each phase depends on the temperature distribution in the other (except in special case where the interface is totally reflecting ($t_{LS} = 0$)). To obtain a solution, therefore, in this complex system, the method of successive iterations was applied as follows.

For a zeroth approximation, a temperature distribution is assumed in both media (for example, by neglecting the radiation), $\tilde{\theta}_{S0}(\tau)$ and $\tilde{\theta}_{L0}(\xi)$. Since the integrations required in the evaluation of the radiative fluxes are quite complex and time consuming to perform by any iterative method of solution, the following alternative procedure was employed. The fourth-

power of the assumed temperature distributions are fitted to a polynomial of the form:

$$\tilde{\theta}^4_{So}(\tau) = \sum_{i=0}^{n} a_i \tau^i, \qquad \tilde{\theta}^4_{Lo}(\xi) = \sum_{i=0}^{n} b_i \xi^i$$

where the coefficients, a_i and b_i, are determined by a best-fit, least-squares, procedure. The integrals of the form $\int \theta^4(\eta)\, E_2(\tau - \eta)\, d\eta$ therefore obtain the form

$$\sum_{i=0}^{n} \int \eta^i\, E_2(\tau - \eta)\, d\eta$$

which can be analytically integrated since:

$$\int x^m E_n(ax + b)\, dx = -\sum_{i=0}^{m} \frac{m!}{(m-i)!} \frac{x^{m-i}}{a^{i+1}} E_{n+i+1}(ax + b) \quad (18)$$

for $m \geqslant 0$ and where a and b are constants. As a result, $F^*_L(\xi)$ and $F^*_S(\tau)$ can be completely determined for the assumed solutions. With the value of q^*_L corresponding to the assumed solutions, the conservation of energy equation in the liquid (equation (14)) can then be numerically integrated by any of the available methods for solving first order, non-linear, differential equations (Runge–Kutta, Adams–Moulton, Kurra–Merson, etc.). Integration is initiated at the interface where the temperature is known (equation (15b)) and continued to τ_L. The deviation of $\theta_L(\tau_L)$ from the boundary condition value of unity (equation (15c)) is used to correct the derived normalized temperature at every point; i.e., zero correction at the interface increasing linearly with distance to the total deviation at $\xi = \tau_L$. This deviation also provides an improved value of the total flux, q^*_L, for the next iteration. As a first approximation, the improved solution for the liquid temperature is substituted into the expression for F^*_L directly. Maintaining the assumed solid temperature distribution, the integrals are evaluated and the differential equation re-solved.† This type of iterative scheme is continued until one obtains convergence, at all points, of successive iterations to the desired accuracy. However, we have found that an alternate procedure, which greatly shortens the convergence time, is to extrapolate (or interpolate) between two successive approximations to obtain the improved approximation for the dimensionless temperature at any point. Once convergence is obtained for the liquid, the solid temperature distribution is obtained in much the same manner except that in this case the total flux, q^*_S, is known from the conservation boundary condition (equation (15a)). Therefore, one must converge, by iteration, only on the temperature in the solid while keeping the liquid temperature fixed. The problem is not, however, complete even after convergence is obtained in the solid since the liquid temperature solution depends on the solid distribution through J^*_L (equation (17b)). With the improved solid solution, the liquid conservation equation must again be solved and this procedure continued until convergence occurs simultaneously in both phases.

Before proceeding with the actual results, it is perhaps important to mention that the existence and uniqueness of solutions of such non-linear, integro-differential equations were discussed and shown in [3] and [4].

3. RESULTS

(a) *General presentation*

In this section, the results for the illustrative example outlined above are presented. These results are given in terms of the dimensionless parameters identified in Table 1 so that they are, with appropriate data, applicable to a variety of particular systems. Each of the physical parameters which were found important in

† It has been found that convergence is improved by averaging the zeroth-approximation and the improved zeroth-approximation to provide the trial solution for the next iteration.

understanding the effects introduced by radiation are varied via the appropriate dimensionless variables. In Table 2, a summary of the physical parameters to be studied are shown as are the corresponding physical parameters which were varied. The data for the reference case used is given in the lower portion of Table 2. Only the mathematical parameters of interest were varied relative to the standard, to obtain the individual results.

Table 2. Physical parameters and corresponding mathematical parameters varied

Physical parameter varied	Parameters of mathematical problems	Figure number
t_{SL}	t_{SL}	3
$\varkappa_S$	τ_S	4
T_M	θ_M	5
$\varkappa_L$	τ_L, τ_∞	6
L_S	$\tau_S, N, L_L/L_S$	7
L_L	$\tau_L, L_L/L_S$	8

Data for reference case

$\tau_S = 0{\cdot}8$	$L_L/L_S = 0{\cdot}5$
$\tau_L = 0{\cdot}5$	$\theta_M = 0{\cdot}8$
$\tau_\infty = 5$	$G_c^* = 0{\cdot}01$
$N = 5$	$t_{GS} = 1{\cdot}0$
	$t_{LS} = 0{\cdot}8$
	$n_S^* = n_S/n_L = 1{\cdot}33$
	$k_S^* = k_S/k_L = 2{\cdot}0$

The results of this investigation are presented in graphical form in Figs. 3–8. The numerical method of integration employed was the Kutta-Merson technique [5] with a convergence criterion for successive iterations of less than 1 per cent. In each case, the "a" figures are the temperature distributions with the insert relating the change of the interface gradient in the liquid $(d\theta_L/dz^*)_i$ and the total flux in the solid (q_S^*) with the parameters describing the parameter being varied. The net dimensionless flux and the dimensionless gradients of the interface, in both the solid and the liquid, are tabulated in Table 3. Each of the "b" figures are the net

Table 3. Calculated temperature gradients at the solid–liquid interface for simultaneous radiative and conductive heat transfer

Identification	Corresponding to Fig.	q_S^*	$\left(\frac{d\theta_L}{dz^*}\right)_i$	$\left(\frac{d\theta_S}{dx^*}\right)_i$
Standard (see Table 2)	3–8	2·51	0·34	−0·33
$t_{LS} = 0$	3	1·18	0·54	−0·52
$t_{LS} = 0{\cdot}4$	3	1·87	0·43	−0·42
$\tau_S = 0{\cdot}5$	4	2·71	0·31	−0·30
$\tau_S = 1{\cdot}0$	4	2·42	0·35	−0·34
$\tau_S = 2{\cdot}0$	4	2·19	0·38	−0·38
$\theta_M = 0{\cdot}85$	5	1·75	0·29	−0·27
$\theta_M = 0{\cdot}90$	5	1·78	0·27	−0·23
$\tau_L = 0{\cdot}25$	6	2·58	0·30	−0·28
$\tau_L = 1{\cdot}0$	6	2·13	0·35	−0·35
$\tau_S = 0{\cdot}5$	7	1·62	0·33	−0·20
$\tau_S = 1{\cdot}0$	7	3·11	0·34	−0·41
$\tau_L = 0{\cdot}25$	8	3·42	0·24	−0·46
$\tau_L = 1{\cdot}0$	8	1·78	0·53	−0·26

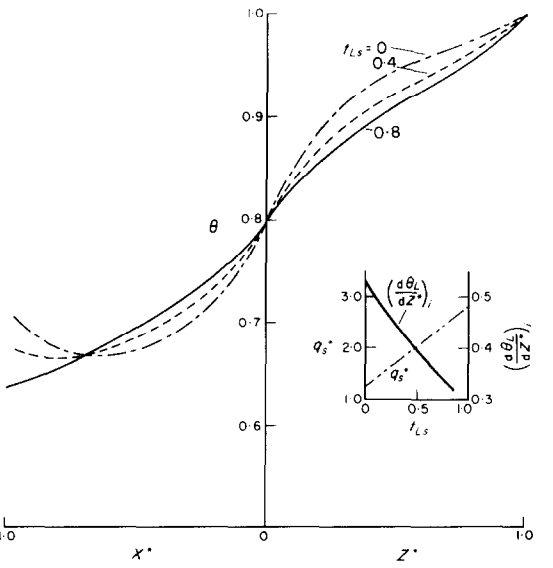

FIG. 3(a). Temperature distributions for simultaneous heat transport by radiation and conduction for a solid in intimate contact with its melt—shows effects of varying the transmittance of the interface. Insert gives dimensionless interface temperature gradient in the liquid and net dimensionless flux.

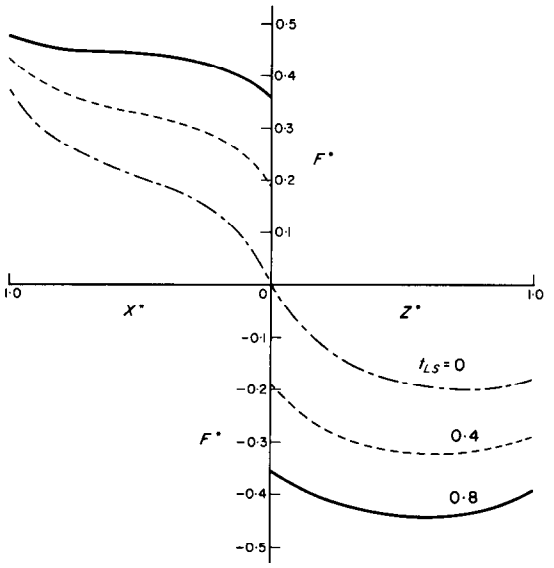

FIG. 3(b). Net dimensionless radiative fluxes corresponding to Fig. 3(a).

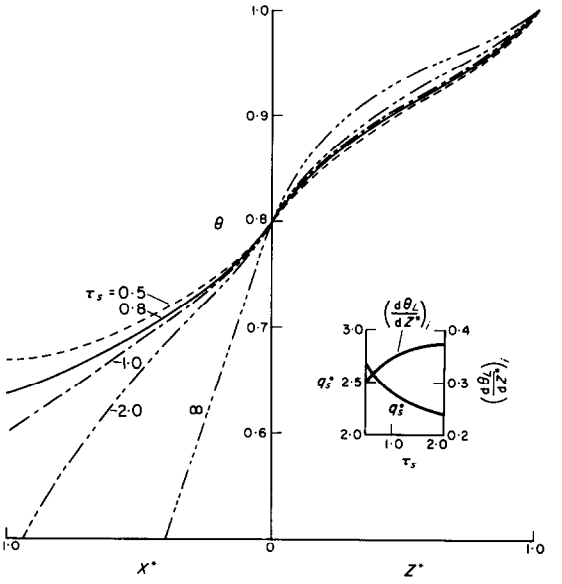

FIG. 4(a). Temperature distributions for simultaneous heat transport by radiation and conduction for a solid in intimate contact with its melt—shows effects of varying the absorptance of the solid phase.

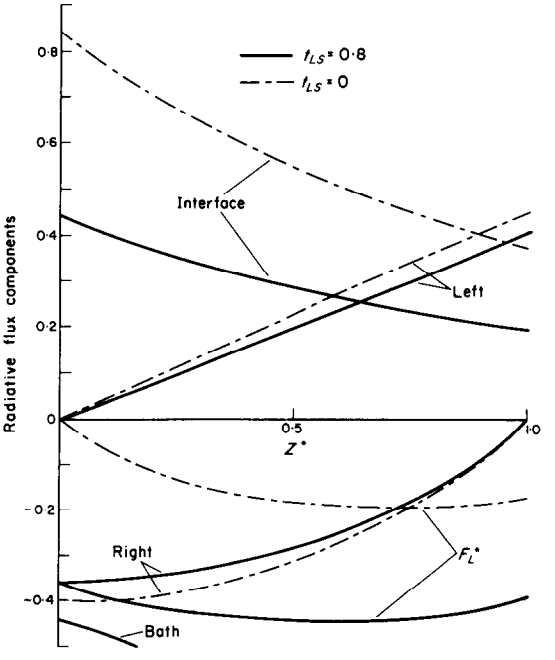

FIG. 3(c). Radiative flux components in the liquid corresponding to Fig. 3(b).

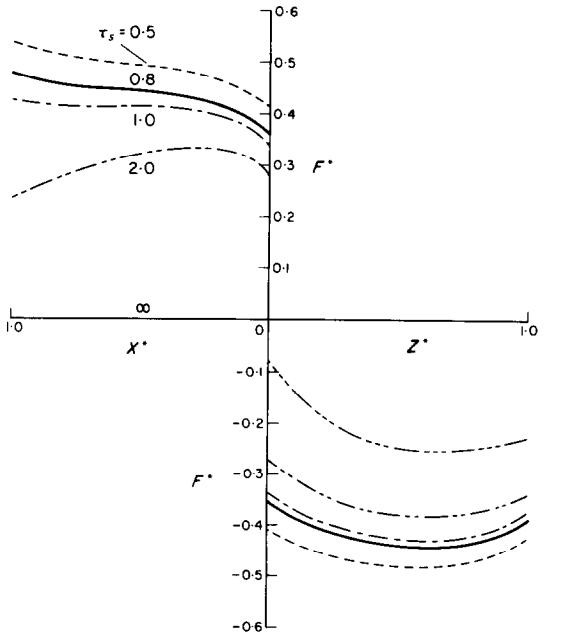

FIG. 4(b). Net dimensionless radiative fluxes corresponding to Fig. 4(a).

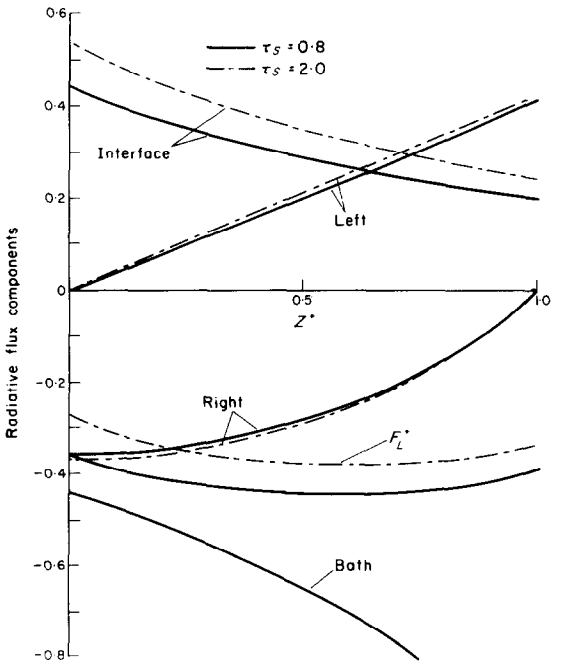

FIG. 4(c). Radiative flux components in the liquid corresponding to Fig. 4(b).

dimensionless radiative fluxes corresponding to the respective temperature distributions. The conductive flux can, of course, be obtained by substitution of q^* and F^* in the energy conservation equations. The net radiative fluxes for certain cases have been decomposed into their component parts (see equations (16) and (17)) and the results presented in the "c" figures. The labels right, left, etc., in these figures indicate the source of the particular flux relative to any arbitrary plane in the media. These c-plots will be used in the discussion section below to interpret the temperature and flux curves of parts "a" and "b". Although, in certain cases, several dimensionless parameters were varied simultaneously, the temperature and flux curves use only one of the variables for identification (e.g., for Fig. 6, τ_L and τ_∞ were both varied by variation of κ_L but in this case $\tau_\infty = 10\tau_L$). The other parameter values for each case, where not obvious, can be obtained by simple calculation or from the insert of the "a" figures. For convenience, the type of line used in each figure is consistent throughout.

(b) *Discussion*

The particular model which is being considered was chosen so that direct comparisons could be made between systems having different combinations of optical properties for the two contacting media. One is free to arbitrarily select the interface temperature (at $x^* = z^* = 0$) as well as the optical properties in both media. In general, the net flux, q^*, in the system is therefore determined by the interface temperature and the optical properties of liquid (see Fig. 2), the temperature of the solid/gas interface adjusting accordingly. As a result of this freedom to constrain the conditions in the liquid, the temperature in the solid is occasionally found to

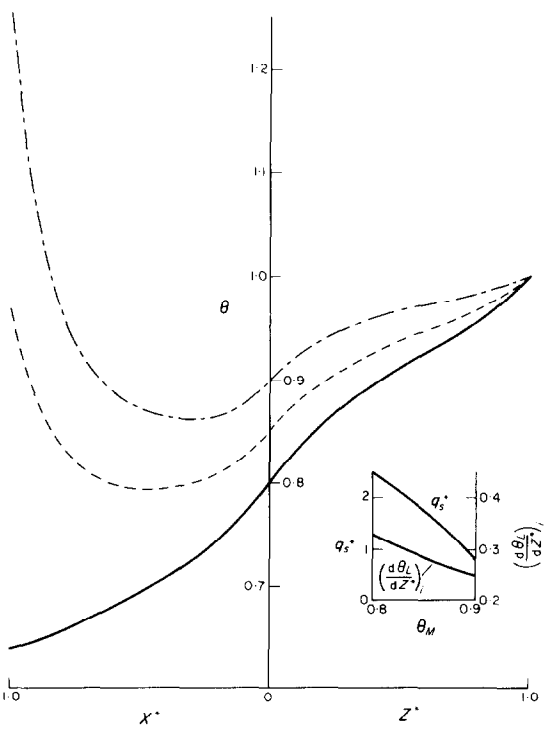

FIG. 5(a). Temperature distributions for simultaneous heat transport by radiation and conduction for a solid in intimate contact with its melt—shows effects of varying the melting temperature relative to the far field liquid temperature.

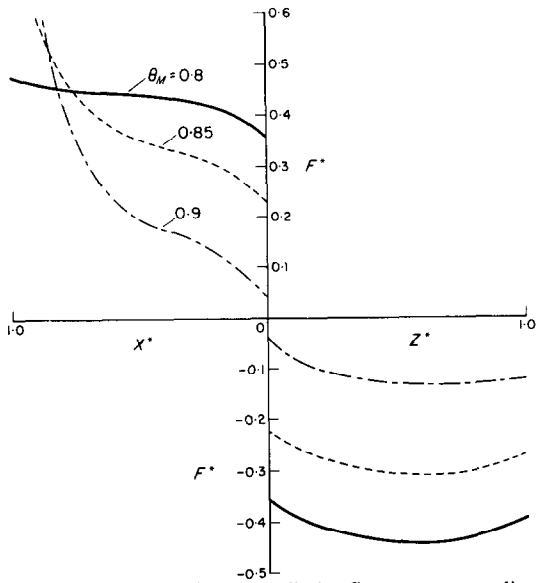

FIG. 5(b). Net dimensionless radiative fluxes corresponding to Fig. 5(a).

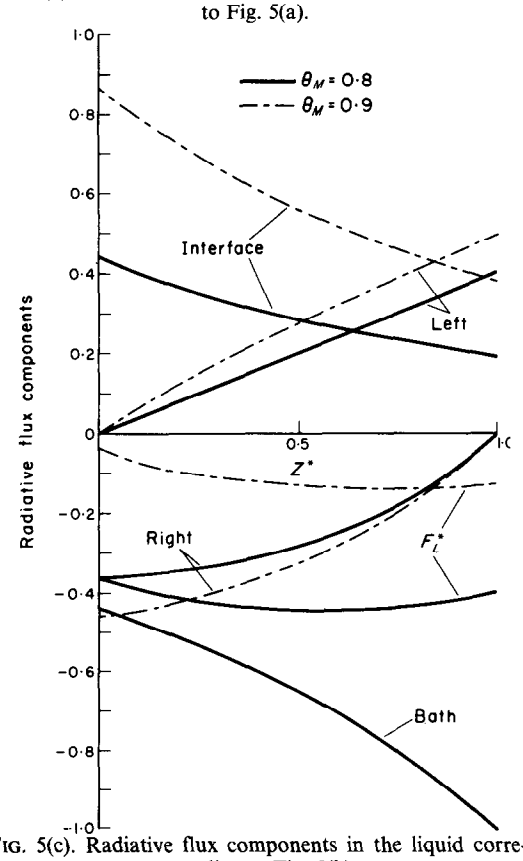

FIG. 5(c). Radiative flux components in the liquid corresponding to Fig. 5(b).

exceed the temperature of the heat source, i.e. the liquid bath for $z^* \geqslant 1$. This is a violation of the Second Law of Thermodynamics and, therefore, such results are to be ignored since they must correspond to situations which are grossly removed from physical reality.

The physical principal which must be remembered in trying to interpret the results of these calculations is the use of steady state conditions. In such circumstances, the net energy flux must be a constant throughout the medium which requires that each of the participating modes of heat transfer compensate for the others in such a way as to maintain the sum a constant. An immediate application of this constraint is to explain the temperature minimum which occurs in the solid in certain cases. In the results where this minimum is observed, changes in the properties of the liquid have forced a decrease in the net flux. To account for this, a negative conductive flux is required in the solid wherever

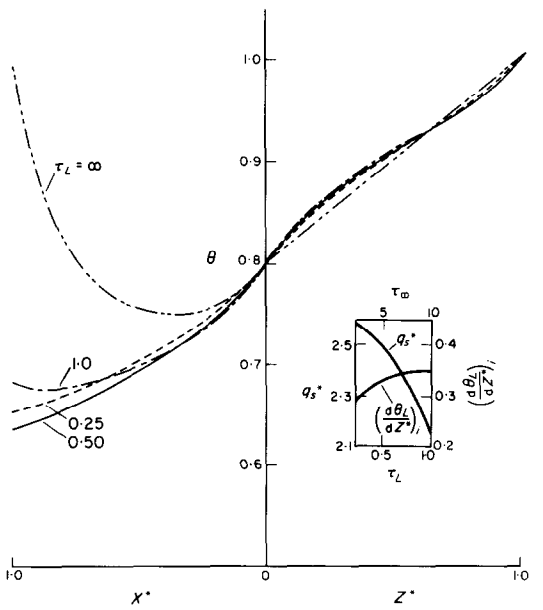

FIG. 6. Temperature distributions for simultaneous heat transport by radiation and conduction for a solid in intimate contact with its melt—shows effect of varying the absorptance of the liquid phase.

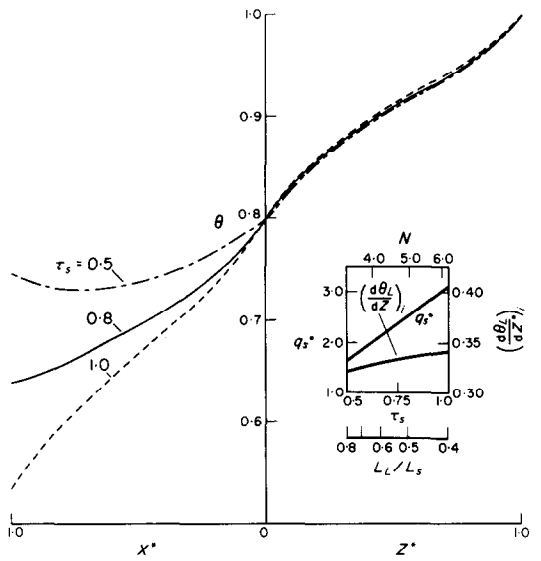

FIG. 7. Temperature distributions for simultaneous heat transport by radiation and conduction for a solid in intimate contact with its melt—shows effect of varying crystal (solid) length.

the optical parameters of this phase require that the radiative flux be larger than the total flux. Although the constancy of energy flux does, in general, explain most of the trends observed in the results, careful examination of each of the graphs provides more detailed understanding of the radiative effects.

In dealing with transparent materials, because the radiative emission increases with the fourth power of the absolute temperature, it is apparent that the radiative flux resulting from regions of high temperature will exceed that from regions of relatively lower temperature. Therefore, in dealing with a material which has a temperature gradient superimposed on it, the radiative flux from the higher temperature region will exceed the flux from the low temperature region. The higher temperature region therefore acts as a source of heat to the lower temperature region. With respect to the over-all shape of the temperature distribution, particularly in the second phase, one must consider the net flux which is determined by the optical properties of the first phase. For the illustrative example, this is so because for all calculations, the boundary temperatures in the liquid (first phase) have been specified and thus the net flux is determined by the liquid phase.

For example, consider Fig. 3 where we have varied the transmittance of the solid/liquid interface from totally reflecting ($t_{LS} = 0$) to 80 per cent transparent ($t_{LS} = 0{\cdot}8$). In this case, the boundary temperatures were fixed at $\theta_M = 0{\cdot}8$ and unity for the interface and the bulk liquid boundary, respectively. As t_{LS} is decreased, the net radiative flux is decreased because of the increased magnitude of the reflected term (see Fig. 3(c)). In accordance with the earlier results of Viskanta and Grosh [2] as the net radiative flux decreases the corresponding temperature distributions are observed to become more convex downward. With respect to the

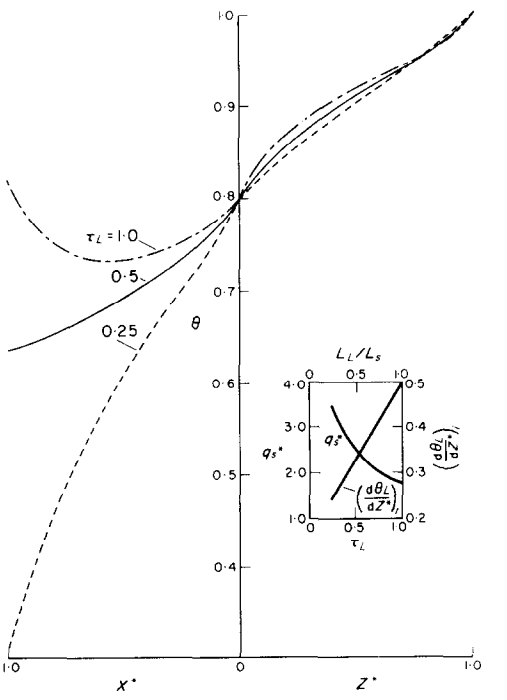

FIG. 8. Temperature distributions for simultaneous heat transport by radiation and conduction for a solid in intimate contact with its melt—shows effect of varying the boundary layer thickness.

solid phase, q_S^* must also decrease as t_{LS} is decreased. However, since the optical properties of the solid have not been changed, a large radiative flux builds up as $x^* \to 1{\cdot}0$. Only through the development of a negative temperature gradient and, thus, a negative conductive flux can the radiative term be counteracted to restrict q_S^* to a small, constant, value throughout the solid. Had there been a large reflected term from the gas/solid interface, the temperature would not develop a minimum in the solid for $t_{LS} = 0$.

An apparent contradiction, with respect to the development of a temperature minimum in the solid as q^* decreases, occurs in Fig. 4 where the optical thickness τ_S of the solid phase has been varied. This, however, is understandable since the magnitude of q^* is being constrained by the properties of the solid not the liquid as in Fig. 3.

The mathematical procedure for the special case of the solid phase being completely opaque ($\tau_S = \infty$) requires further discussion.† The solid no longer permits any heat transport by radiation and thus the energy conservation equation for that phase becomes that of pure conduction. Radiation emitted in the solid (proportional to T_S^4) is immediately attenuated by the adjacent layers since the absorption coefficient is infinite for a finite physical thickness. However, the atoms in the solid phase at the interface emit half their total energy into the partially transparent liquid phase. Therefore, there must still be a term in the radiative flux for the liquid phase which is transmitted from the surface of the opaque solid phase. One may obtain the value from the general term of equation (17), i.e.

$$t_{LS} n_S^{*2} \int_0^{\tau_S} \theta_S^4(\eta)\, E_2(\eta)\, \mathrm{d}\eta$$

by considering that $\theta_S(\tau) = \theta_M$ when $\tau_S = \infty$. Thus:

$$t_{LS} n_S^{*2} \theta_M^4 \int_0^{\infty} E_2(\eta)\, \mathrm{d}\eta = t_{LS} n_S^{*2} \theta_M^4/2 \qquad (19)$$

which is in direct accord with the above physical argument. In this special case, the transmittance (t_{LS}) is directly analogous to the emittance (ϵ) which one would have anticipated in the results, since $\alpha = \epsilon$ and $\alpha + r = 1$.

Another interesting feature of Fig. 4, which requires explanation and again shows the importance of considering the flux component curves, is the shift in the liquid temperature distribution as the optical thickness of the solid increases. This change coincides with a decrease in the net radiative flux in the liquid (Fig. 4(b)). Examination of the individual flux components shows that the term which contributes most to the reduction of the radiative flux in the liquid is the component of the interface term which is transmitted from the solid; i.e.

$$2 t_{LS} n_S^{*2} \int_0^{\tau_S} \theta_S^4(\eta)\, E_2(\eta)\, \mathrm{d}\eta.$$

(The difference in the reflected fluxes which also affects the net interface term between $\tau_S = 0{\cdot}5$ and $\tau_S = 2{\cdot}0$ is negligible. This can be verified by the small change in area under the curves labeled "right" which are, in turn, further decreased in magnitude by the reflectance $r_{LS} = 0{\cdot}2$). This result is understandable since, for any specific temperature distribution in the solid, as τ_S increases, i.e. as the solid becomes more opaque, it must emit more radiation. Mathematically, the above term increases since the magnitude of the integral increases between the limits 0 and τ_S, as the optical thickness in the solid increases. The larger is the value of τ_S, the larger is the average temperature over the region of integration.

In Fig. 5, the results of increasing the melting temperature relative to the far field are seen to be consistent with the discussion above, both mathematically and physically. As the interface temperature approaches that of the far field, the difference in the radiative flux between the high and low temperature regions decreases. This is shown by the decreasing net radiative

† The mathematical procedure outlined here is analogously applicable for the liquid phase being opaque and the solid being partially transparent.

flux in the liquid (Fig. 5(b)) as θ_M increases. The reason for this decrease in radiative flux as the interface temperature approaches that of the bath is clear upon examining the component radiative fluxes given in Fig. 5(c). The figure shows the large increase in the interface term as θ_M increases. This is primarily caused by the larger flux transmitted from the solid which is now at relatively higher temperatures. Since no changes are made in the physical properties of the solid, that phase must develop a temperature minimum in order to satisfy equation (13) and the gradient becomes negative to oppose the large F_S^* which develops as $x^* \to 1{\cdot}0$.

In the remaining results presented, Figs. 6–8, only the temperature distributions are given. The variation in the radiative fluxes are in accordance with the fluxes given in the insert. All of the observed details can be explained in terms of the rationale employed above. It is important, in interpreting these results, to remember that the problem has been formulated in dimensionless parameters and the presented results are not always directly indicative of the physical variations. Comparison, in these cases, must be made by converting the data to the appropriate dimensional form.

4. SUMMARY

The equations for conservation of thermal energy for two contacting absorbing media experiencing steady state heat transport were derived, from the more general conservation equations, for a model which simulates a crystal growing from its own melt. The numerical method of solution was discussed and the results presented as a series of dimensionless temperature and flux distributions for various combinations of optical and physical parameters. The interpretation of these results, which should be indicative of any two such contacting media, is found to be greatly facilitated by decomposing the net radiative flux into its component parts. Qualitatively, the consequences of the radiative flux can be understood with the aid of the component flux curves and recalling that the assumption of steady state requires the total flux to be constant throughout the system.

ACKNOWLEDGEMENTS

We wish to extend our gratitude to Professor W. A. Tiller for his valuable comments and interest in this study. Partial support by the U.S. Air Force Office of Scientific Research, Grant AF-AFOSR 731-65, is acknowledged.

REFERENCES

1. R. VISKANTA, Radiation transfer and interaction of convection with radiation heat transfer, *Advances in Heat Transfer* (Edited by T. F. Irvine and J. P. Hartnett), Vol. 3, pp. 175–251. Academic Press, New York (1966).
2. R. VISKANTA and R. J. GROSH, Heat transfer by simultaneous conduction and radiation in an absorbing medium, *Trans. Am. Soc. Mech. Engrs*, (C) *J. Heat Transfer* **84**, 63–72 (1962).
3. L. LICHTENSTEIN, *Vorlesungen über einige Klassen Nichtlinearen Integral-gleichungen and Integro-Differential-gluchungen*. Springer-Verlag, Berlin (1931).
4. P. M. ANSELONE (Editor), *Non-linear Integral Equations*. The University of Wisconsin Press, Madison, Wisconsin (1964).
5. L. FOX, *Numerical Solution of Ordinary and Partial Differential Equations*, p. 24. Pergamon Press, Oxford (1962).

Résumé—Le transport d'énergie par conduction et rayonnement simultanés entre deux milieux en contact intime est considéré en insistant principalement sur la formulation mathématique du flux de rayonnement. Pour obtenir une certaine connaissance des effets introduits par un transport par rayonnement, le formidable problème général est simplifié en une diffusion unidimensionnelle en régime permanent entre deux milieux partiellement transparents en contact thermique intime. La méthode numérique de résolution des équations intégrodifférentielles couplées et non-linéaires qui en résultant est décrite en détail. Les résultats sont présentés sous la forme d'une série de la température dimensionnelle et des distributions de flux correspondantes pour un grand nombre de propriétés optiques et physiques. L'interprétation de ces résultats est donnée à la fois sur la base d'un raisonnement physique et par rapport à la formulation mathématique.

Zusammenfassung—Es wird der Energietransport betrachtet bei gleichzeitiger Leitung und Strahlung zwischen zwei Medien in innigem Kontakt, wobei das Hauptgewicht auf die mathematische Formulierung der Strahlungsverhältnisse gelegt ist. Um Kenntnis von jenem Einfluss zu erhalten, der vom Strahlungsaustausch herrührt, wird das komplexe allgemeine Problem auf die eindimensionale, stationäre Übertragung zwischen zwei teilweise transparenten Medien in innigem thermischen Kontakt zurückgeführt. Die numerische Lösungsmethode für die resultierenden, gekoppelten, nicht-linearen Integral-Differentialgleichungen ist im einzelnen beschrieben. Die Ergebnisse sind wiedergegeben als eine Reihe von Temperatur- und entsprechenden Stromverteilungen für eine Vielzahl von optischen und physikalischen Eigenschaften. Eine Auslegung dieser Ergebnisse erfolgt sowohl auf Grund physikalischer Überlegungen als auch im Hinblick auf die mathematische Formulierung.

Аннотация—Рассматривается кондуктивно-радиационный энергообмен между двумя контактирующими средами, причем упор делается на математическую запись лучистого потока. Чтобы понять вызванные лучистым теплообменом эффекты, общая задача сводится к одномерной установившейся диффузии между двумя частично прозрачными средами, находящимися в непосредственном тепловом потоке. Подробно описывается численный метод решения выведенных нелинейных интегро-дифференциальных уравнений. Результаты представлены в виде рядов размерной температуры и соответствующих распределений потока с учетом различных оптических и физических свойств. Дана физическая и математическая интерпретация результатов.